

Supporting Information

Composition engineering of $\text{Cu}_2\text{ZnGe}_x\text{Sn}_{1-x}\text{S}_4$ nanoparticles hole transport layer for carbon electrode-based perovskite solar cells

Nian Cheng^{a*}, Weiwei Li^a, Zhenyu Xiao^b, Han Pan^a, Dingshan Zheng^a, and Wen-Xing Yang^{a*}

^a School of Physics and Optoelectronic Engineering, Yangtze University, Jingzhou 434023, China

^b Energy-Saving Building Materials Collaborative Innovation Center of Henan Province, Xinyang Normal University, 237 Nanhu Road, Xinyang 464000, China

*Corresponding author

Email: chengnian@foxmail.com, wenxingyang2@126.com

1. Experimental section

1.1 Synthesis of $\text{Cu}_2\text{ZnGe}_x\text{Sn}_{1-x}\text{S}_4$ nanoparticles

$\text{Cu}_2\text{ZnGe}_x\text{Sn}_{1-x}\text{S}_4$ nanoparticles ($x = 0, 0.25, 0.50, 0.75, \text{ and } 1.0$) are synthesized according to the procedures in our previous reports[1, 2]. In brief, 4 mmol $\text{CuCl}_2 \cdot 2\text{H}_2\text{O}$, 2 mmol ZnCl_2 , $2x$ mmol GeCl_4 , and $2(1-x)$ mmol SnCl_2 are weighed and added into a three-neck flask. Then 20 mL oleylamine is also added into the flask. The flask is connected to a Schlenk line, and evacuated using a vacuum pump. The flask is heated up to 130 °C to completely dissolve the reactants. 8 mmol sulfur powder is dissolved into 10 mL oleylamine in another bottle, and then added into the above flask. Once again, the flask is evacuated using a vacuum pump, and then filled with flowing Ar gas.

Then, the flask is heated to 230 °C, and kept at this temperature for 60 min. When the reaction is finished, the obtained $\text{Cu}_2\text{ZnGe}_x\text{Sn}_{1-x}\text{S}_4$ nanoparticles are thoroughly washed using n-hexane and ethanol for six times, then dried in a vacuum oven at 70 °C for 24 h.

1.2 Fabrication of carbon electrode-based perovskite solar cells

The patterned FTO substrates are thoroughly washed via ultrasonication in deionized water and ethanol in sequence, and dried at 100 °C before used. SnO_2 electron transport layer is prepared via spin-coating a precursor solution containing tin oxalate in proper amount of hydrogen peroxide and deionized water, and heat-treated at 180 °C for 30 min[3]. The perovskite film is prepared using a two-step spin-coating method[3-5]. First, 1.3 M PbI_2 in mixed DMF/DMSO (950 μL : 50 μL) is spin-coated onto the SnO_2 electron transport layer, and then dried at 70 °C for 1 min. Then 60 mg FAI, 6 mg MABr, and 6 mg MACl in 1 mL isopropanol is spin-coated onto the PbI_2 film, and annealed at 150 °C for 15 min. $\text{Cu}_2\text{ZnGe}_x\text{Sn}_{1-x}\text{S}_4$ nanoparticles ink is prepared by dispersing 100 mg $\text{Cu}_2\text{ZnGe}_x\text{Sn}_{1-x}\text{S}_4$ nanoparticles in 1 mL hexanethiol, and then spin-coated onto the perovskite film at 4000 rpm for 30 s, and dried at 100 °C for 60 min. The carbon electrode is doctor-bladed onto the $\text{Cu}_2\text{ZnGe}_x\text{Sn}_{1-x}\text{S}_4$ hole transport layer, and dried at 100 °C for 30 min.

1.3 Characterizations

The $\text{Cu}_2\text{ZnGe}_x\text{Sn}_{1-x}\text{S}_4$ nanoparticles are first characterized using X-ray diffraction (XRD, SmartLab 9 kW), Raman (Lab-RAM), and transmission electron microscope (TEM, Hitachi S4800) to confirm their crystal structure, phase purity, and crystal

morphology. Morphologies of the two-step deposited perovskite film and spin-coated $\text{Cu}_2\text{ZnGe}_x\text{Sn}_{1-x}\text{S}_4$ hole transport layer on perovskite film are observed using scan electron microscope (SEM, Regulus 8220). Energy band positions of the $\text{Cu}_2\text{ZnGe}_x\text{Sn}_{1-x}\text{S}_4$ hole transport layer are evaluated using ultraviolet photoelectron spectroscopy (UPS, Escalab 250Xi). Photoluminescence (PL) and time-resolved photoluminescence (TRPL) of the perovskite/ $\text{Cu}_2\text{ZnGe}_x\text{Sn}_{1-x}\text{S}_4$ bilayer films are further characterized using FLS980. Current density-voltage (J-V) curves of FTO/ $\text{Cu}_2\text{ZnGe}_x\text{Sn}_{1-x}\text{S}_4$ /Carbon devices are measured in dark condition using Keithley 2450 sourcemeter from 0 V to 1.0 V.

J-V curves of the carbon electrode-based perovskite solar cells are measured using Keithley 2450 sourcemeter. The simulated AM 1.5G solar light (100 mW cm^{-2}) is provided using a solar simulator (XEF-300). Effective area of the perovskite solar cell is kept to 0.04 cm^2 using a metal mask. The IPCE spectrum of perovskite solar cell is measured using a commercial QE-R instrument. The stability of the perovskite solar cell is tested for 30 days without capsulation, during this period, the perovskite solar cell is stored in the dry air with humidity around 20%, and its J-V curves are measured in the ambient atmosphere with humidity around 30~40% every 5 days. Capacitance-voltage (C-V), electrochemical impedance at 1.0 V under dark condition, and dark J-V curves of the carbon electrode-based perovskite solar cells are measured using a CHI760E workstation.

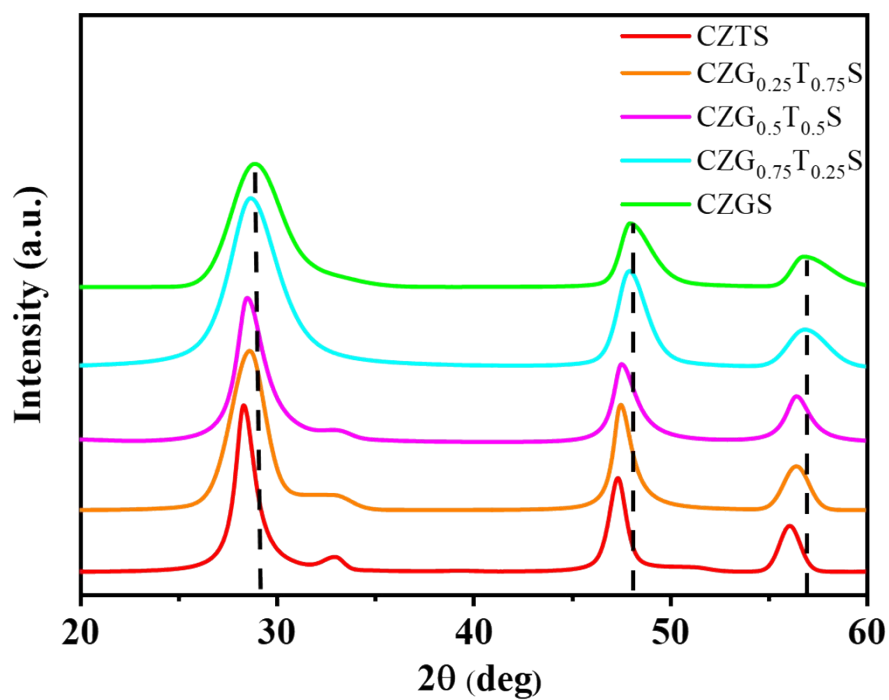


Figure S1. XRD patterns for all $\text{CZG}_x\text{T}_{1-x}\text{S}$ samples ($x = 0.0, 0.25, 0.50, 0.75,$ and 1.0).

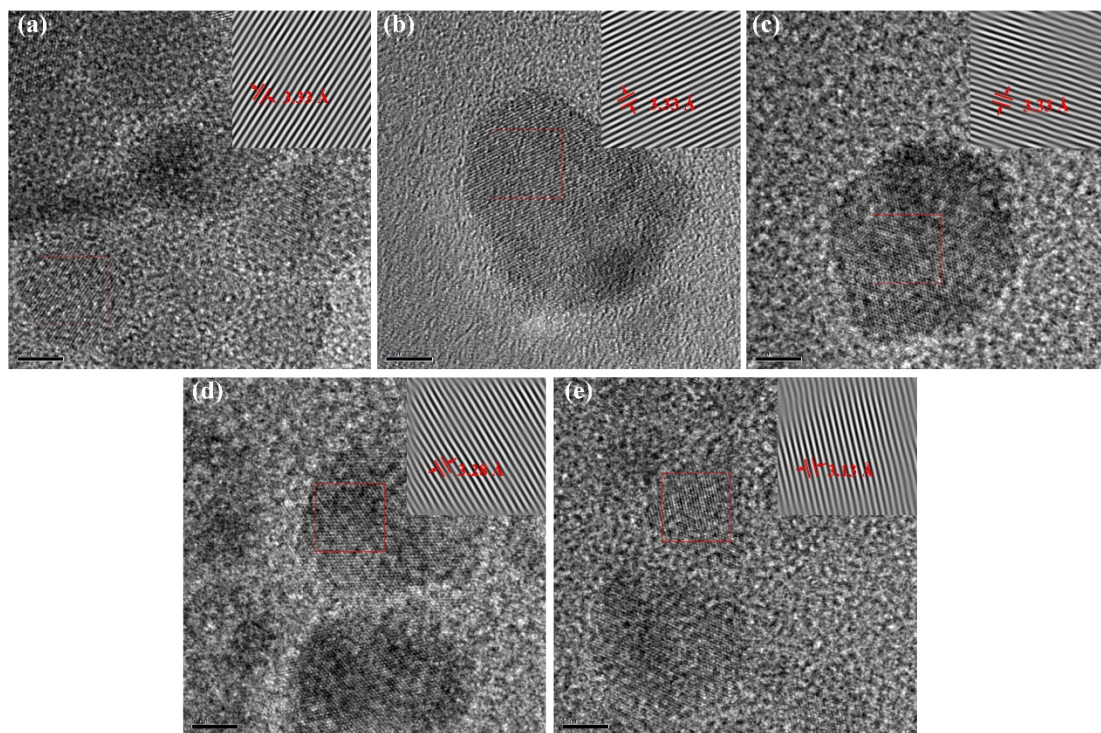


Figure S2. HRTEM images of (a) CZTS, (b) $\text{CZG}_{0.25}\text{T}_{0.75}\text{S}$, (c) $\text{CZG}_{0.5}\text{T}_{0.5}\text{S}$, (d) $\text{CZG}_{0.75}\text{T}_{0.25}\text{S}$, and (e) CZGS nanoparticles. The lattice distances are determined from

the inverse FFT figures.

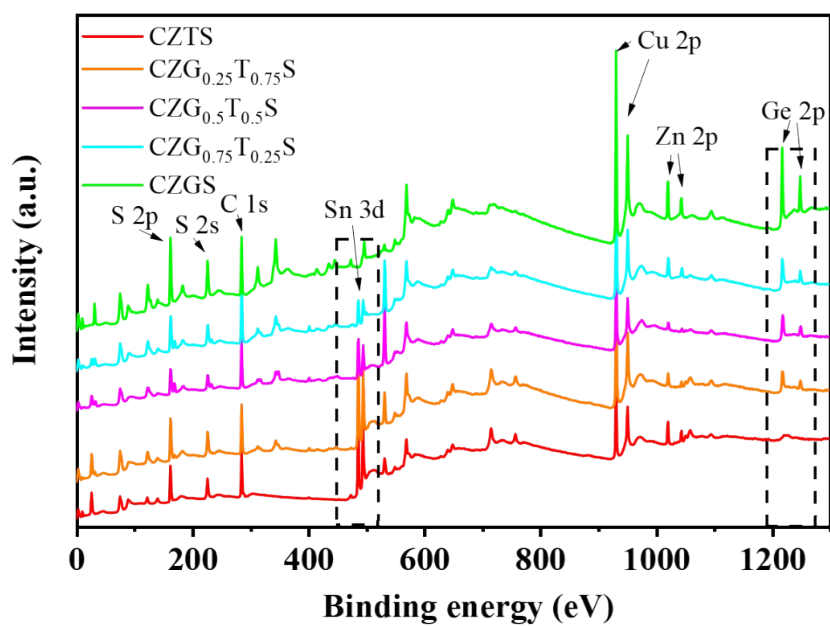


Figure S3. Full XPS survey spectra for all $\text{CZG}_x\text{T}_{1-x}\text{S}$ samples ($x = 0.0, 0.25, 0.50, 0.75,$ and 1.0).

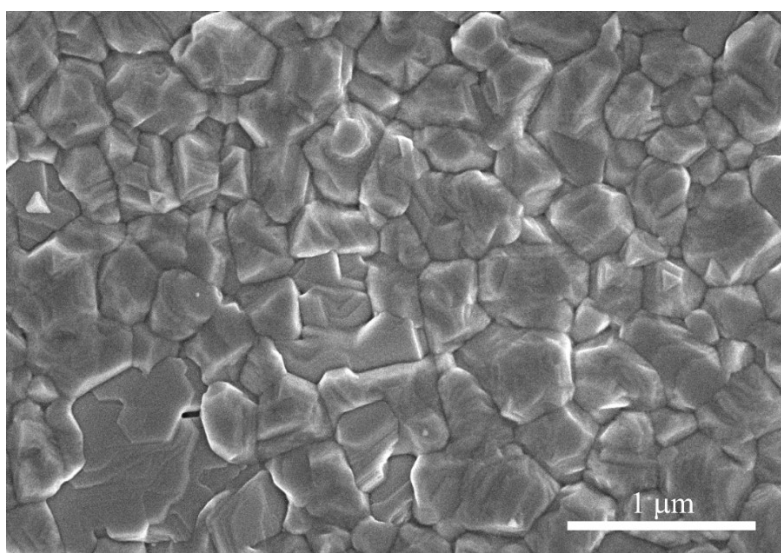


Figure S4. Planar SEM image of FAPbI_3 perovskite film prepared via two-step deposition method.

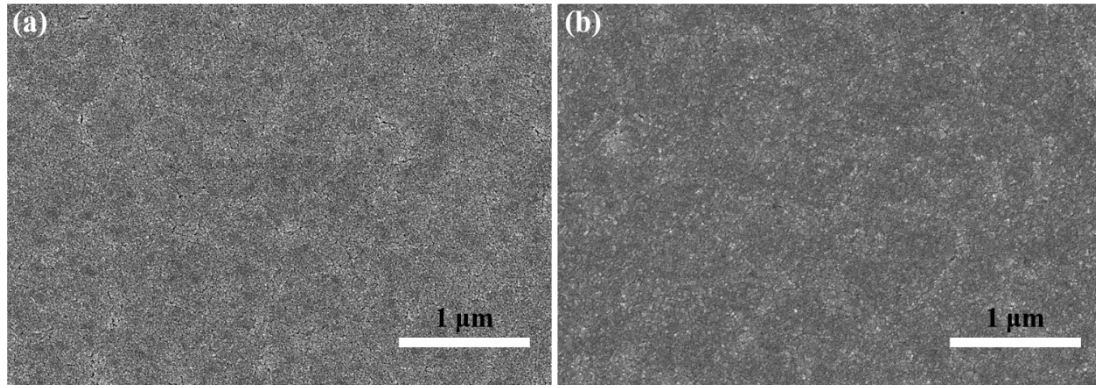


Figure S5. Planar SEM images of (a) $\text{CZG}_{0.25}\text{T}_{0.75}\text{S}$ and (b) $\text{CZG}_{0.75}\text{T}_{0.25}\text{S}$ HTL films deposited onto perovskite films.

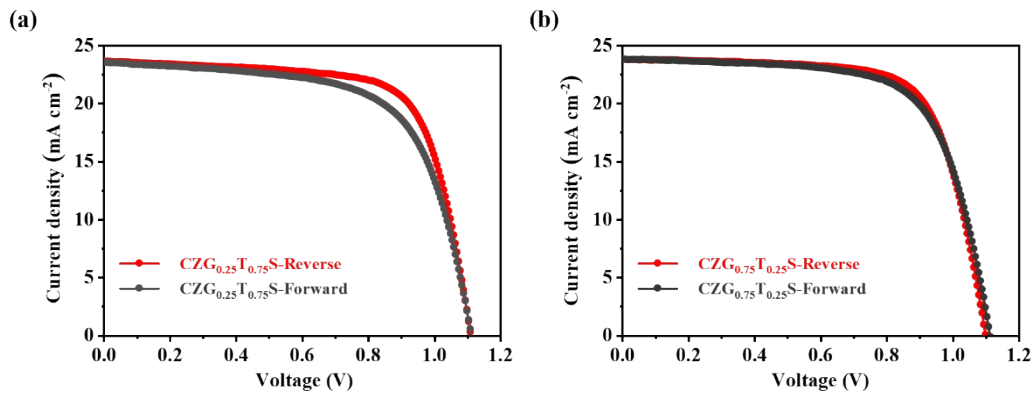


Figure S6. Champion J-V curves for C-PSCs with $\text{CZG}_{0.25}\text{T}_{0.75}\text{S}$ and $\text{CZG}_{0.75}\text{T}_{0.25}\text{S}$ HTLs. The champions PCEs are 18.60% ($V_{\text{oc}} = 1.110$ V, $J_{\text{sc}} = 23.66$ mA cm⁻², FF = 70.82%) and 18.63% ($V_{\text{oc}} = 1.102$ V, $J_{\text{sc}} = 23.82$ mA cm⁻², FF = 70.96%) for $\text{CZG}_{0.25}\text{T}_{0.75}\text{S}$ and $\text{CZG}_{0.75}\text{T}_{0.25}\text{S}$ HTLs respectively.

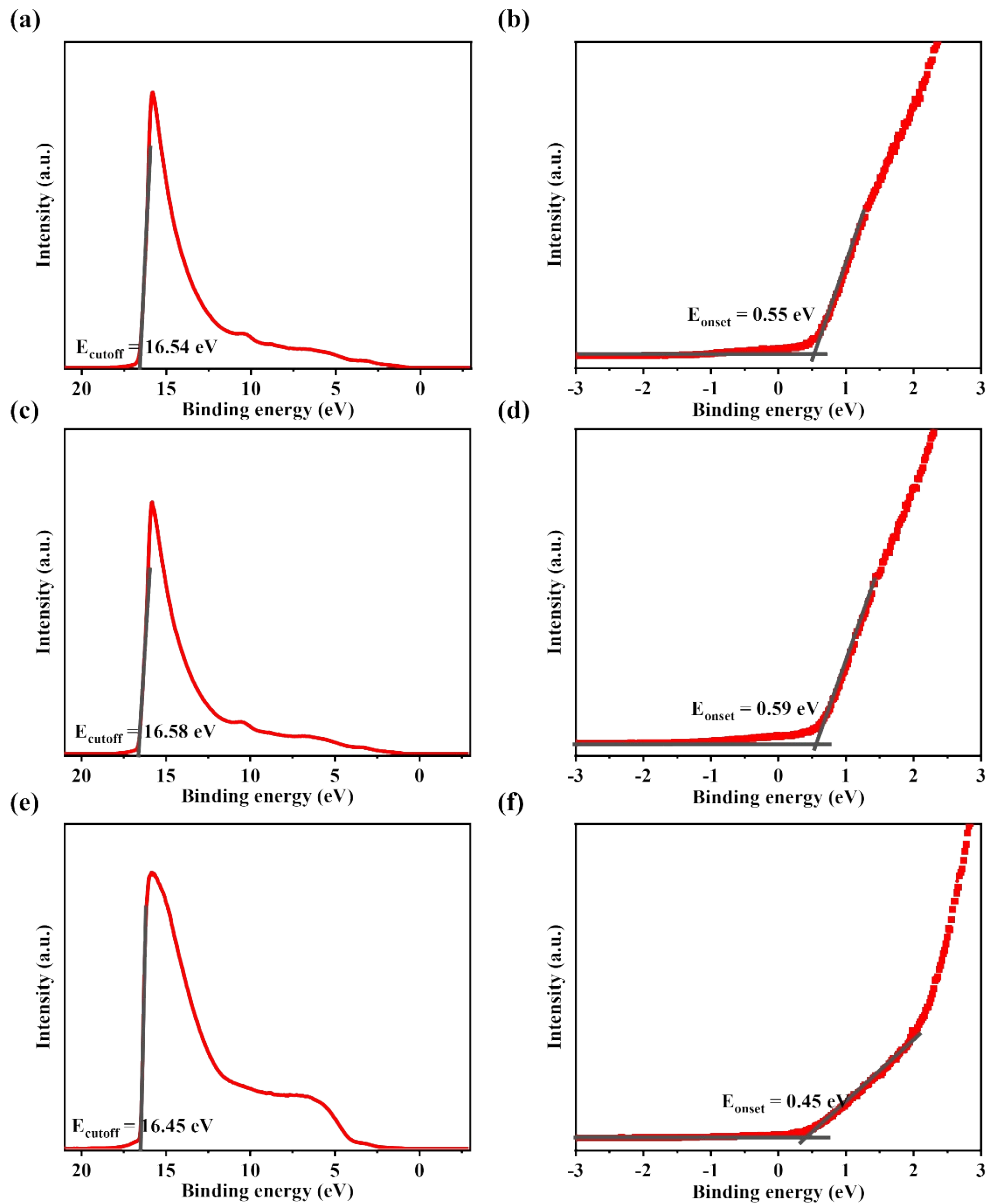


Figure S7. UPS spectra of $\text{CZG}_x\text{T}_{1-x}\text{S}$ HTL. (a) and (b) CZTS HTL, (c) and (d) $\text{CZG}_{0.5}\text{T}_{0.5}\text{S}$ HTL, (e) and (f) CZGS HTL. The valence band position (E_{VB}) is calculated using equation $E_{\text{VB}} = -(\text{h}\nu - E_{\text{cutoff}} + E_{\text{onset}})$, where $\text{h}\nu$ is the energy of the UPS light source (21.22 eV).

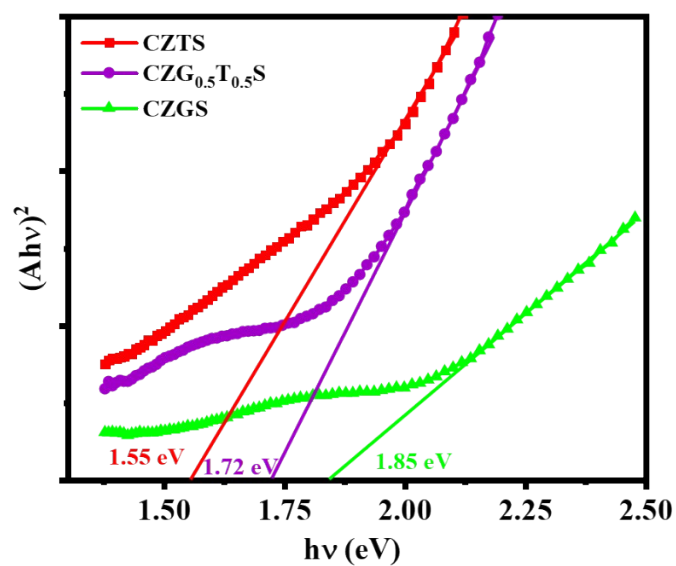


Figure S8. Tauc plots for CZTS, CZG_{0.5}T_{0.5}S, and CZGS HTLs. The estimated band gaps for CZTS, CZG_{0.5}T_{0.5}S, and CZGS HTLs are 1.55 eV, 1.72 eV, and 1.85 eV respectively.

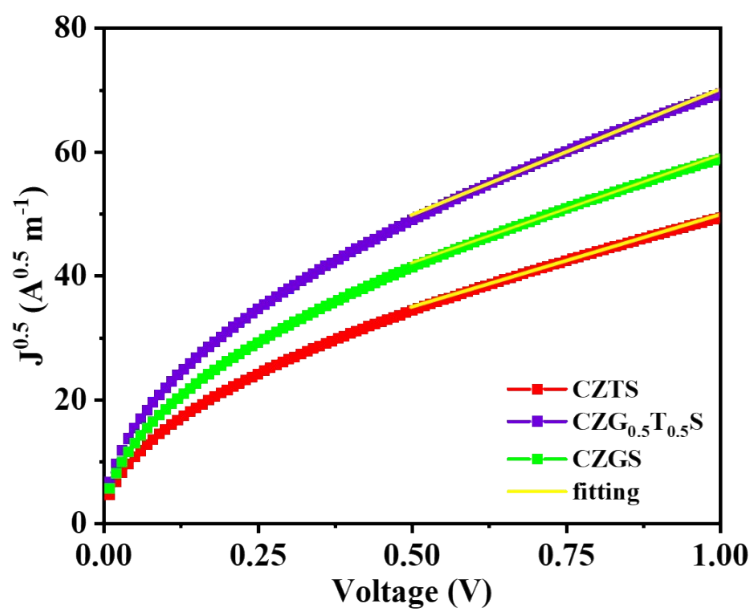


Figure S9. $J^{1/2}$ versus voltage curves of CZG_xT_{1-x}S HTLs. The curves are fitted between 0.5 V and 1.0 V.

Table S1. Summary of XRD diffraction peaks and lattice constants for CZG_xT_{1-x}S samples.

	(112) peak (degree)	(204) peak (degree)	(312) peak (degree)	a (Å)	c (Å)
CZTS	28.34	47.38	56.12	5.48	10.792
CZG _{0.5} T _{0.5} S	28.50	47.56	56.48	5.43	10.790
CZGS	28.88	48.00	56.86	5.35	10.705

Table S2. Atomic percentages of Cu, Zn, Sn, Ge and S atoms for CZG_xT_{1-x}S samples from EDS measurements.

	Cu (atom%)	Zn (atom%)	Sn (atom%)	Ge (atom%)	S (atom%)
CZTS	33.16	14.57	12.72	0.0	39.55
CZG _{0.25} T _{0.75} S	34.07	13.81	9.30	2.68	40.14
CZG _{0.5} T _{0.5} S	35.79	15.26	7.29	7.55	34.11
CZG _{0.75} T _{0.25} S	32.66	15.19	3.56	10.35	38.24
CZGS	30.60	12.43	0.0	9.13	47.83

Table S3. Summary of V_{oc}, J_{sc}, FF, and PCE for C-PSCs with different CZG_xT_{1-x}S HTLs.

	V _{oc} (V)	J _{sc} (mA cm ⁻²)	FF (%)	PCE (%)
CZTS	1.037±0.006	22.77±0.40	68.71±1.02	16.22±0.31
CZG _{0.25} T _{0.75} S	1.092±0.017	23.71±0.20	70.96±0.66	18.36±0.12
CZG _{0.50} T _{0.50} S	1.136±0.010	24.14±0.13	71.35±0.77	19.57±0.17
CZG _{0.75} T _{0.25} S	1.102±0.012	23.62±0.16	70.24±0.79	18.28±0.26
CZGS	1.066±0.014	23.29±0.26	69.20±1.01	17.17±0.24

Table S4. Summary of the fitting parameters for the TRPL spectra using a double-exponential decay function.

	A_1	t_1 (ns)	A_2	t_2 (ns)	t_{avg} (ns)
Perovskite	626.77	24.8	376.09	283.4	250.5
CZTS	778.99	19.9	221.85	85.6	56.0
CZG _{0.5} T _{0.5} S	749.54	18.0	250.33	60.0	40.1
CZGS	753.35	17.9	252.79	66.6	44.9

References

1. Cheng, N., Liu, Z., Li, W., Yu, Z., Lei, B., Zi, W., Xiao, Z., Sun, S., Zhao, Z. and Zong, P.-A., *Cu₂ZnGeS₄ as a novel hole transport material for carbon-based perovskite solar cells with power conversion efficiency above 18%*. Chemical Engineering Journal, 2023. **454**.
2. Liu, Z., Yu, Z., Li, W., Zhao, Z., Xiao, Z., Lei, B., Zi, W., Cheng, N., Liu, J. and Tu, Y., *Scalable one-step heating up synthesis of Cu₂ZnSnS₄ nanocrystals hole conducting materials for carbon electrode based perovskite solar cells*. Solar Energy, 2021. **224**:51-57.
3. Cheng, N., Yu, Z., Li, W., Liu, Z., Lei, B., Zi, W., Xiao, Z., Tu, Y. and Rodríguez-Gallegos, C.D., *Highly efficient perovskite solar cells employing SnO₂ electron transporting layer derived from a tin oxalate precursor solution*. Journal of Power Sources, 2022. **544**.
4. Cheng, N., Li, W., Zheng, D. and Yang, W.-X., *Enhance the efficiency of perovskite solar cells using W doped SnO₂ electron transporting layer*. ChemPhotoChem, 2024.
5. Cheng, N., Li, W., Zheng, D. and Yang, W.X., *Surface Passivation of Perovskite Solar Cells with Oxalic Acid: Increased Efficiency and Device Stability*. ChemPlusChem, 2023. **88**(10).

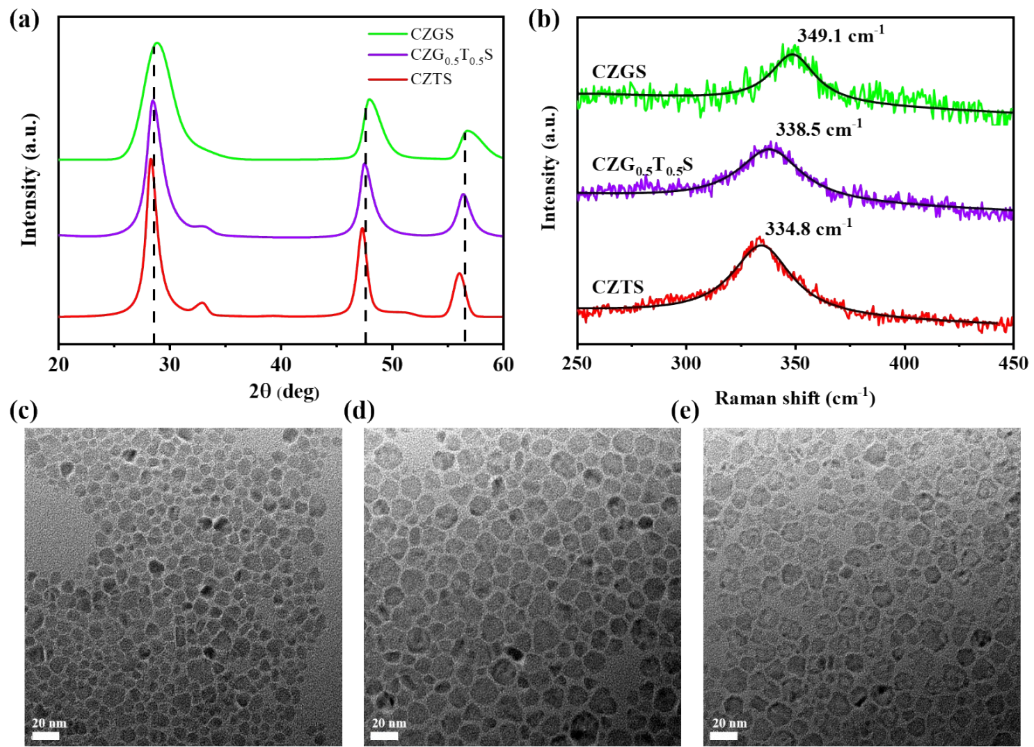


Figure 1. (a) XRD patterns and (b) Raman spectra for $\text{CZG}_x\text{T}_{1-x}\text{S}$ samples, TEM morphologies of (c) CZTS, (d) $\text{CZG}_{0.5}\text{T}_{0.5}\text{S}$, and (e) CZGS samples.

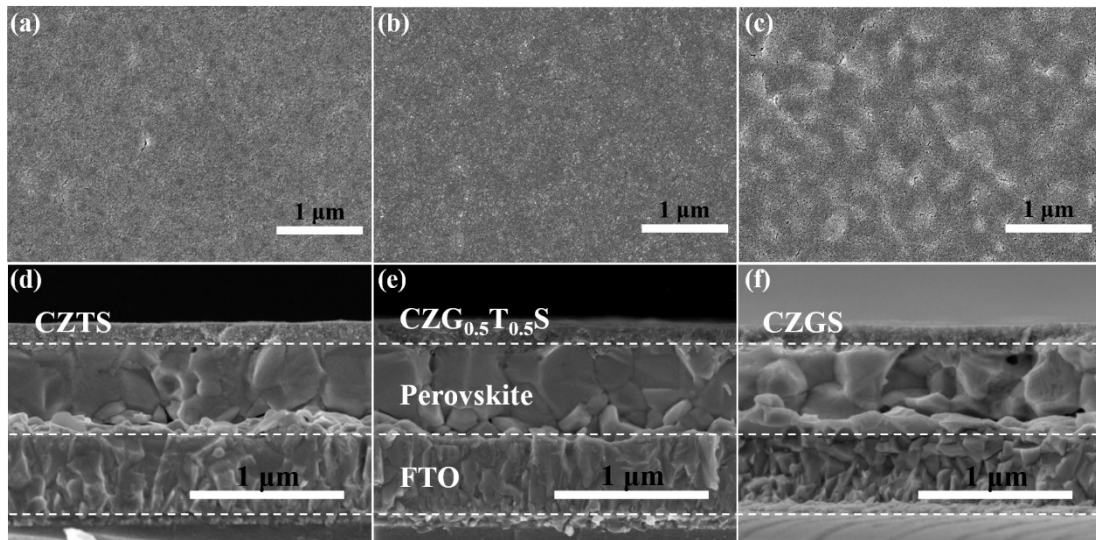


Figure 2. Planar and Cross-sectional SEM images of (a) and (d) CZTS, (b) and (e) $\text{CZG}_{0.5}\text{T}_{0.5}\text{S}$, (c) and (f) CZGS HTLs.

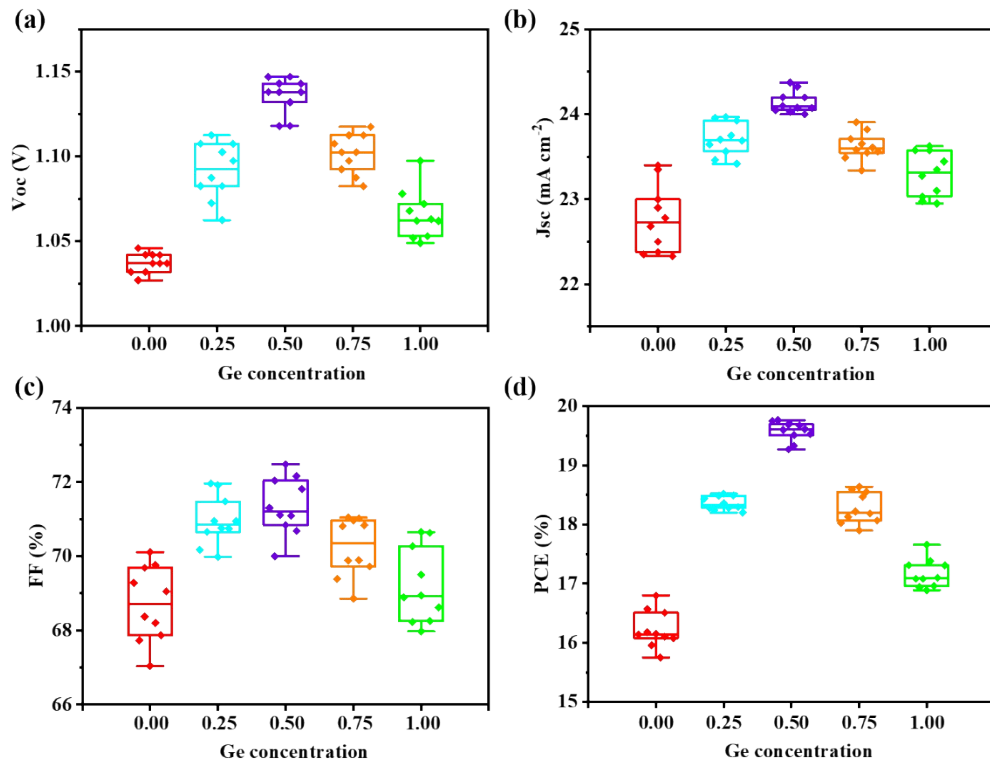


Figure 3. Summary of photovoltaic performances of C-PSCs with different CZG_xT_{1-x}S HTLs (x = 0, 0.25, 0.50, 0.75, and 1.0).

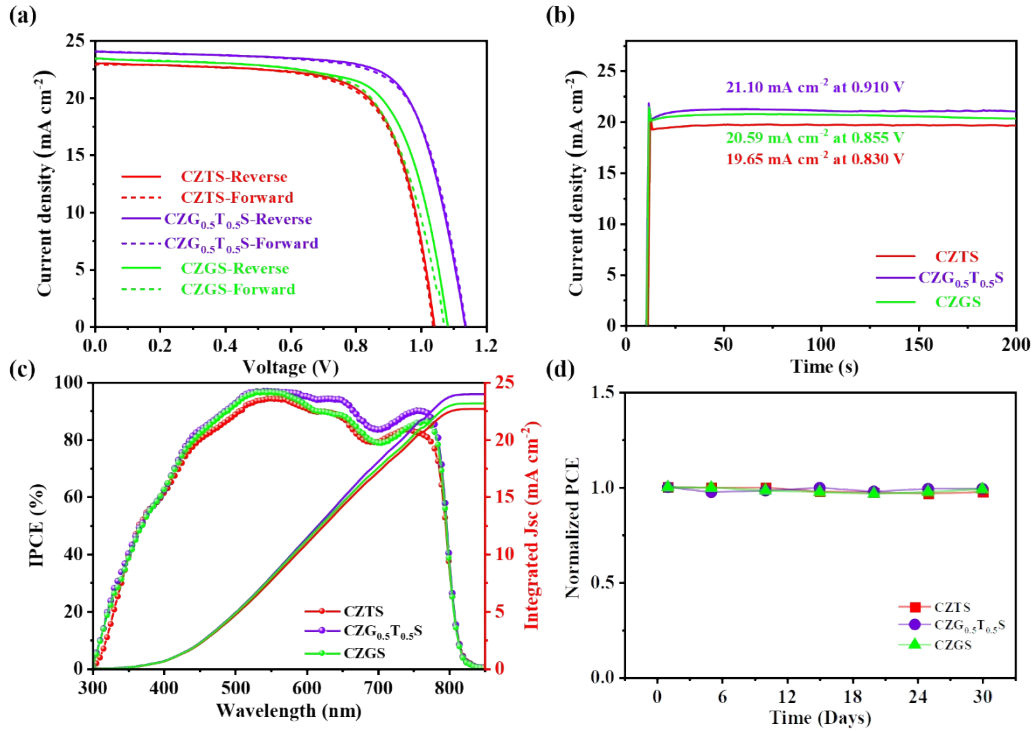


Figure 4. (a) J-V curves, (b) Stable output curves, (c) IPCE spectra, and (d) Device stability for the champion C-PSCs with CZTS, CZG_{0.5}T_{0.5}S, and CZGS HTLs.

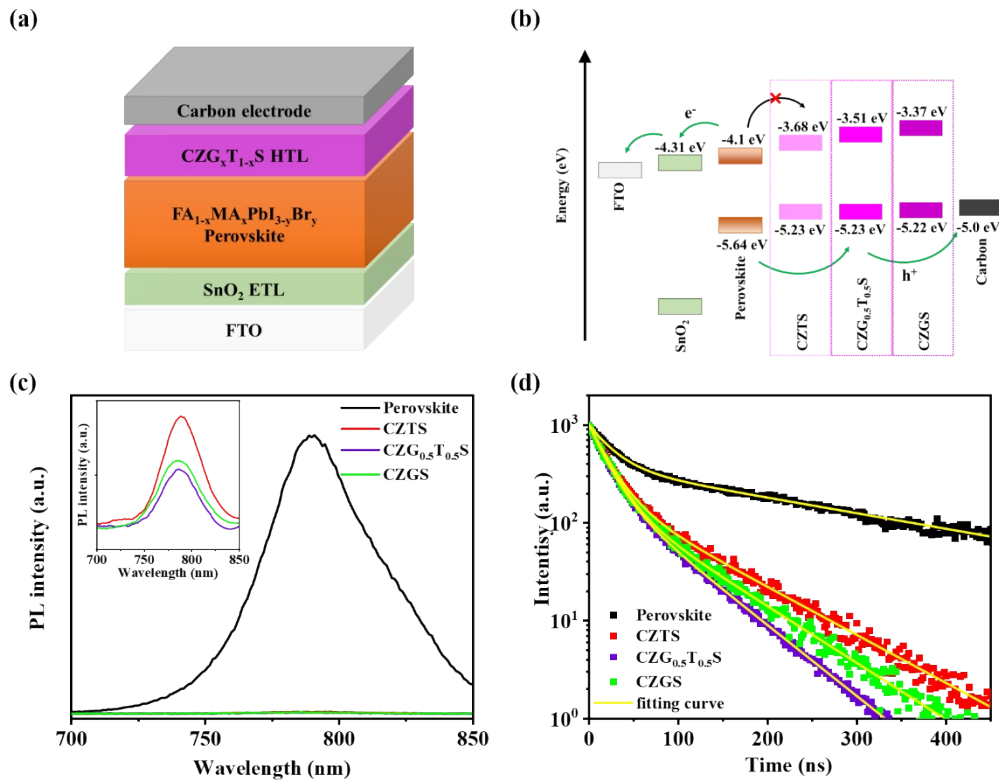


Figure 5. (a) Schematic device structure and (b) Energy band alignment for our C-PSCs, (c) PL and (d) TRPL spectra for perovskite/CZG_xT_{1-x}S (x = 0, 0.5, and 1.0) films.

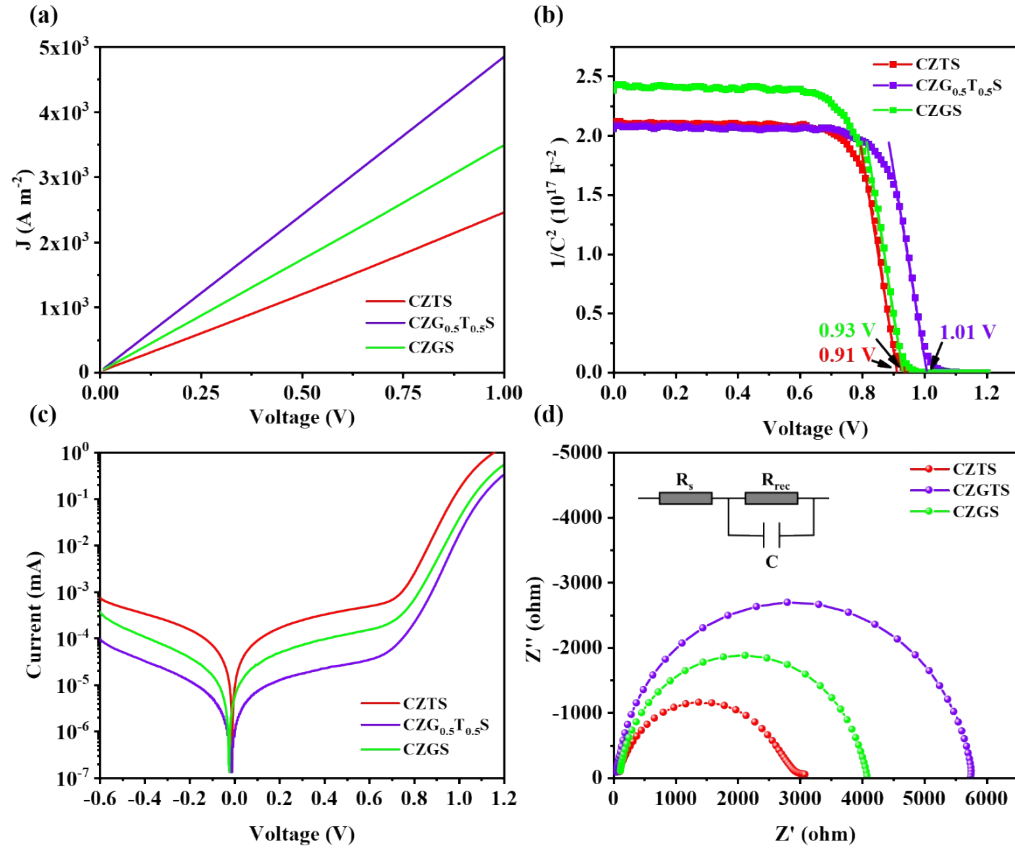


Figure 6. (a) J-V curves of CZG_xT_{1-x}S HTLs, (b) Mott-Schottky curves, (c) Dark current-voltage curves, and (d) EIS spectra of C-PSCs with CZG_xT_{1-x}S HTLs (x = 0, 0.5, and 1.0).